WATER SURFACE CONDITION AND TWO CHANNEL MICROWAVE MEASUREMENTS

K. Tsuchiya*, S. Yamamoto, C. Ishida and M. Shimada
National Space Development Agency of Japan (NASDA)
2-4-1, Hamamatu-cho, Minato-ku, Tokyo, 105 Japan

I. Isozaki
Meteorological Research Institute / Meteorological Agency
1-1, Nagamine, Yatabe-cho, Tsukuba-gun, Ibaragi, 305 Japan

Abstract

Passive microwave measurements of water surface of the pool (12 m X 25 m) were made from a 20-m tower in October 1981.
Analysis of the data indicated that correlation between antenna temperature and incident angle was positive for vertical polarization and negative for horizontal polarization. It was found that effect of side lobe can not be neglected. A method of eliminate side lobe effect is described.

1. Introduction

Marine Observation Satellite-1 (MOS-1) is the first Japanese earth observation satellite which will be launched in 1986. Two frequency (23.8 GHz and 31.4 GHz) microwave scanning radiometer (MSR) are to be installed in MOS-1. Making use of a bread board model of MSR, radiation emitted from the water surface was observed at the test site of Meteorological Research Institute. In the experiment, MSR was mounted on a 20-m tower and a 12 m X 25 m pool filled with pure water was used. The objectives of the experiment are to get relationship between antenna temperature and various parameters to make use of the data obtained from the MSR onboard MOS-1 after it is launched.

2. Method of observation

The specification of MSR used the experiment is shown in Table 1. Output signal is integrated for 10 msec and 47 msec simultaneously at the two frequencies. It has a radiometric resolution of 1.0 K at 300 K. As is indicated in the fuctional block diagram of Fig. 1, MSR is consisted of two Dicke type receivers, into which signals are fed by an antenna and calibration sources, delivering analog output signals to an encoder. Observed temperature and calibration source temperature are recorded onto an instrumentation tape together with auxiliary data such as annotation data which are manually input and physical temperature of components of MSR which are necessary for computing wave guide loss for radiometric calibration.

Antenna diameter is 50 cm and detailed antenna pattern measurements were conducted before the experiment for each frequency. Fig. 2 shows MSR atenna patterns at 23.8 GHz and 31.4 GHz.
MSR was installed in a frame with capability of adjustable elevation angle. Polarization is also adjustable by rotating the radiometer about its electrical

* Current affiliation Chiba University
1-33, Yayoi-cho, Chiba-city, 260 Japan

axis thus it is possible to measure antenna temperature of water surface for incident angle ranging from 0° to 40° in both vertical and horizontal polarizations. The experiment was conducted from October 19 through 27,1981 from the top of 20-m height tower.
The coordinate system of the experiment is illustrated in Fig. 3.

3. The results of the analysis of the data

The results of the analysis of observed data indicate the following features

1) Effect of incident angle (Fig. 4)

The correlation between antenna temperature and incident angle was positive for vertical polarization while it was negative for horizontal polarization.

2) Effect of frequency (Fig. 4)

Antenna temperature of 23.8 GHz was lower than that of 31.4 GHz regardless of polarization. This result is opposite to the theoretical characteristics.

3) Variation of antenna temperature associated with polarization (Fig.5)

The variation of antenna temperature associated with changing polarization indicated of sine function.

4) Comparing with the theoretical value

The antenna temperature obtained in this experiment was higher than the theoretical value. The offset value was as large as 40 K.

The facts stated in 2) and 4) suggest necessity of further analysis. The effect of side-lobe is discussed in the following section.

4. Antenna sidelobe correction

In general, the antenna temperature T_A is given by

$$T_A = \frac{\int_{4\pi} T_B\, G(\phi,\theta)\, d\Omega}{\int_{4\pi} G(\phi,\theta)\, d\Omega} \qquad \text{----------(1)}$$

Where T_B is the brightness temperature of the target and $G(\phi\ \theta)$ is the antenna's pattern function, which is the fuction of azimuth and elevation angles ϕ, θ respectively. The contribution of the ground and sky is included in T_A besides the water surface when sidelobe and backlobe effects are taken into account therefore the expression for T_A is expressed by Eq. (2)

$$T_A = \frac{1}{G_0}\left\{\int_{\Omega W} T_{B.W}\, G\, d\Omega + \int_{\Omega s} T_{B.S}\, G\, d\Omega + \int_{\Omega g} T_{B.G}\, G\, d\Omega\right\} \text{-----(2)}$$

Where $T_{B.W}$, $T_{B.G}$ and $T_{B.S}$ are the brightness temperature of the water, ground and sky respectively,where G_0 is the denominator of Eq. (1).

Due to the fact that the size of the pool is comparatively small, $T_{B.W}$ can be assumed to be nearly constant, the estimation of the value of Eq.(2) is reduced to the estimation of the terms $\int_\Omega G\, d\Omega$ for each integration area.

In the actual computation, the magnitude of G, antenna gain was read out at 1/3° interval between 0° and 18°, and 2° interval between 18° and 180°.

Now in the first term $1/G_0 \int_{\Omega W} G\, d\Omega$ signifies the ratio of the contribution of water (pool), to the whole integration area including pool , ground and sky. The similar interpretation is applicable to other two terms.

For the actual computation of $\int_{\Omega} G \, d\Omega$ the following procedures were taken;

1) First term

$$\frac{1}{G_0}\int_{\Omega w} G(\phi\ \theta)\, d\Omega = \frac{1}{G_0}\int_{X_1}^{X_2}\int_{Y_1}^{Y_2} G(X,Y)\frac{Z_a\, dX\, dY}{((X-Xa)^2+(Y-Ya)^2+Za^2)^{3/2}} \quad ----(3)$$

where the suffix"a"denotes the center of the antenna, while X_1 , Y_1 , X_2 and Y_2 are the edges of the pool respectively.

2) Second term

$$\frac{1}{G_0}\int_{\Omega s} G(\phi, \theta)\, d\Omega = \frac{1}{G_0}\int_0^{\pi}\int_0^{\pi} G(\zeta)\sin\theta\, d\theta\, d\phi \quad ----------(4)$$

$$\zeta = \cos^{-1}(\cos\theta\sin\beta - \sin\theta\sin\phi\cos\beta) \quad ---------(5)$$

where β is incident angle.

3) Third term = 1 - (First term + Second term) ----------(6)

The result of the computation is indicated in Table 2. Based on the value in Table 2, Eq. (2) can be easily computed, for example in case of incident angle 10° at 31.4 GHz, the following equation holds.

$$T_A = 0.837\, T_{B.w} + 0.146\, T_{B.G} + 0.017\, T_{B.S} \quad ----------(7)$$

Same rule is applicable to other angle of incident .
In Eq. (7), the value of $T_{B.S}$ was estimated from the graph in Radar Handbook [4.], $T_{B.G}$ was assumed to be 290 K in reference with meteorological observation while T_A is the observed value, thus the value of $T_{B.W}$ is uniquely determined. The values of $T_{B.W}$'s thus obtained for 5 different incident angles are shown in Fig. 6. Comparing Fig. 4 with previously shown Fig.6, it can be seen that the obtained values of $T_{B.W}$'s for different incident angles have good correspondence with those theoretical values. The result of computation for 23.8 GHz also indicates good correspondence with the theoretical values.

It is interesting to notice that the relationship between $(T_{B.W})_{23\ GHz}$ and $(T_{B.W})_{31GHz}$ stated in section 3 - 2) has become opposite after correction, i.e.$(T_{B.W})_{31GHz}$ has become higher than $(T_{B.W})_{23GHz}$.
It should be stated also that large offset value described in 3 - 4) is greatly reduced.

5. Concluding remark

The foregoing analysis leads to the following conclusion. The effect of side lobe is fairly extensive and can not be neglected in such a condition as this experiment. Further experiments at different water surface and meteorological conditions are indispensable to establish reliable data processing algorithm.

References

[1] Hollinger,J.P.,"Microwave Properties of Calm Sea", NRL Rep.7110,1973.
[2] S.T.Wu,et al.,"A Theory of Microwave Apparent Temperature Over the Ocean", NASA CR-2329,1973.
[3] W.M.Truman,et al.,"Three Dimensional Vector Modeling & Restoration of Flat Finite Wave Tank Radiometric measurements", IEEE Tran. Ant.& Prop.,Vol.AP-25 Jan.1977.
[4] King,D.D.,"Passive Detection",Radar Handbook,Chapter 39.
[5] Moore,R.K.,"Microwave Remote Sensing",Manual of Remote Sensing,Chapter 9.

Table 1. Specification of MSR (MOS-1 BBM)

Frequency	23.8 GHz	31.4 GHz
RF Bandwidth	400 MHz	500 MHz
Beam width	1.99 deg.	1.45 deg.
Integration Time	10 & 47 msec	10 & 47 msec
Radiometric Resolution	1.0 K at 300 K	1.0 K at 300 K
Dynamic Range	30 - 330 K	30 - 330 K
Polarization	Horizontal *	Vertical *

* In the field experiment, BBM was modified to dual polarization

Table 2. The ratio of the contribution of each integration area at 31.4 GHz

Incident angle	$\frac{1}{G_0}\int_{\Omega w} T_{B.W}\, G\, d\Omega$	$\frac{1}{G_0}\int_{\Omega s} T_{B.S}\, G\, d\Omega$	$\frac{1}{G_0}\int_{\Omega g} T_{B.G}\, G\, d\Omega$
10°	0.837	0.146	0.017
15°	0.849	0.133	0.018
20°	0.851	0.130	0.019
30°	0.838	0.140	0.022
40°	0.802	0.174	0.024

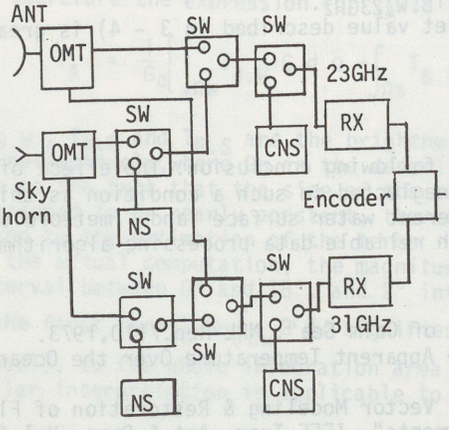

ANT : Antenna
OMT : Orthagonal Mode Transducer
SW : Switch
NS : Noise Source
CNS : Comparison Noise Source
RX : Receiver

Fig.1 Block diagram of MSR

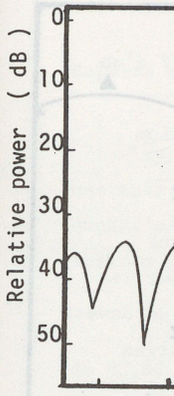

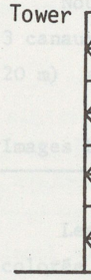

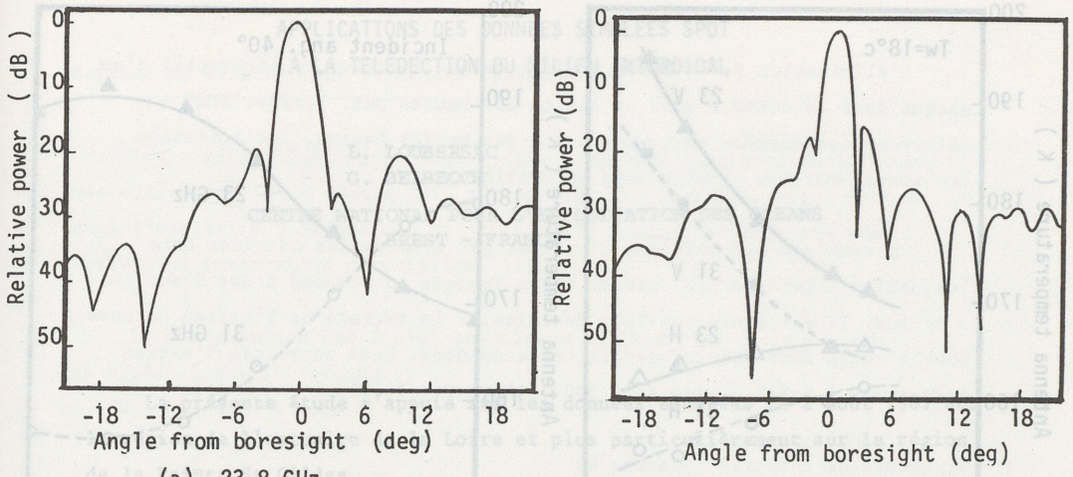

Fig. 2 MSR (MOS-1 BBM) antenna patterns at 23.8 GHz and 31.4 GHz

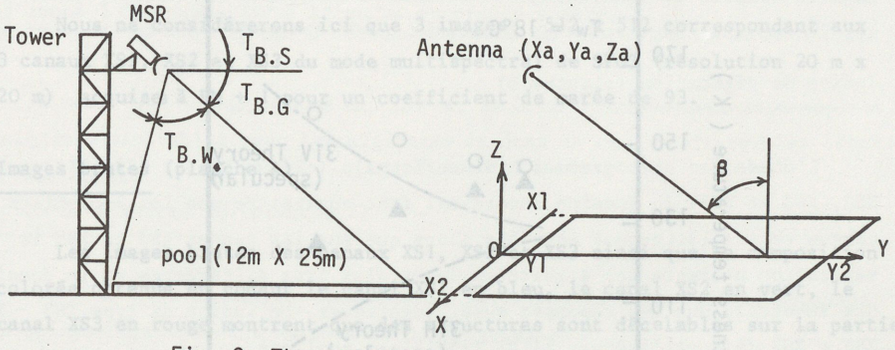

Fig. 3 The coordinate system of the experiment

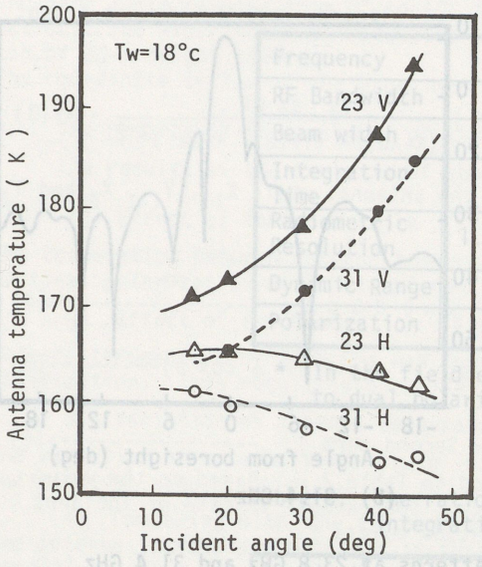

Fig. 4 Incident angle dependence of antenna temperature

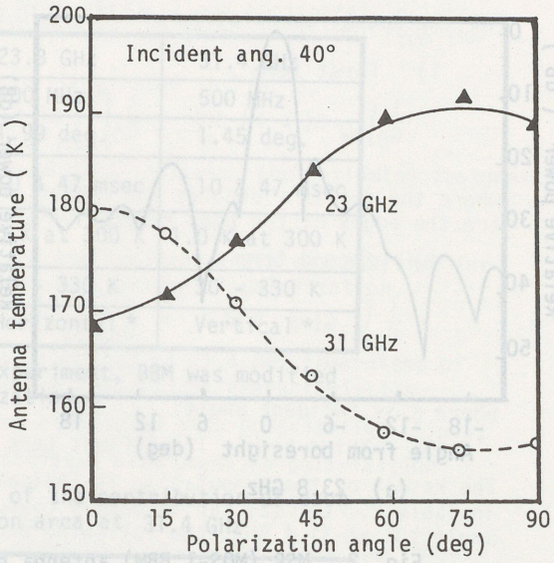

Fig. 5 Polarization angle dependence of antenna temperature

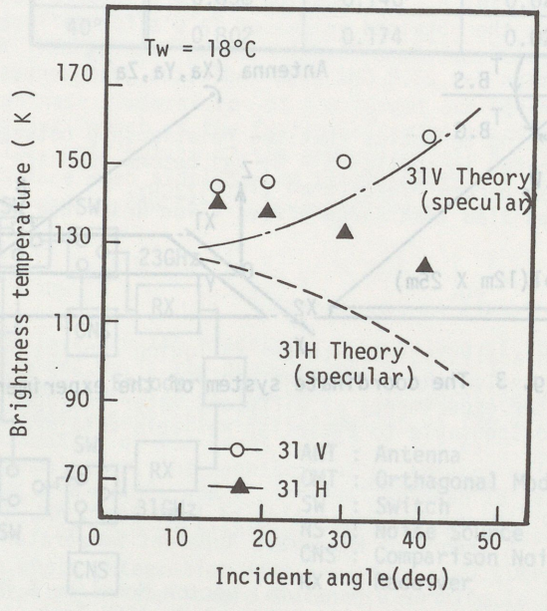

Fig. 6 Incident angle dependence of brightness temperature